

Morphological and luminescent properties of $Y_3(AlGa)_5O_{12}:Ce^{3+}$ powder phosphor.

S T S Dlamini, H C Swart¹ and O M Ntwaeaborwa

Department of Physics, University of the Free State, P. O. Box 339, Bloemfontein, ZA-9300, South Africa

E-mail: SwartHC@ufs.ac.za

Abstract. The morphological and luminescent properties of $Y_3(AlGa)_5O_{12}:Ce^{3+}$ powder phosphor were investigated. Scanning Electron Microscopy revealed the phosphor's agglomerated particles with a size ranging from 0.4 μ to 1.4 μ . The X-ray diffraction indicated a cubic polycrystalline phosphor with an average crystal size of 80 nm. Luminescent properties include the emission wavelength at 512 nm which was also used to approximate the Al/Ga ratio within the crystal. Photoluminescence data also revealed that the addition of the Ga into the YAG:Ce³⁺ matrix caused a blue-shift in the emission spectra. The UV-VUV excitation and emission spectra of the $Y_3(AlGa)_5O_{12}:Ce^{3+}$ were also recorded and an energy diagram was constructed from the values.

1. Introduction

¹Cerium-doped yttrium aluminum garnet ($Y_3Al_5O_{12}:Ce^{3+}$ or YAG:Ce) is used in several applications such as solid state lighting and displays. The Ce³⁺ ion is responsible for a nanosecond decay time and an intense emission at a visible wavelength range. Most phosphors have been developed for the use in fluorescent tubes or compact fluorescent lamps (CFLs) that use UV radiation, but yet they have not been optimized for the use in light emitting diodes (LEDs) that emit in the visible spectrum range. The first basic commercially available white LED is based on an InGaN chip emitting blue light at a wavelength of 460 nm that is coated with a YAG:Ce phosphor layer that converted some of the blue light into yellow light which is combined to a rather cool white light [1]. This is good for many applications (e.g., displays and lighting in cars), but the quality of light is not good enough for home lighting, for which a warmer white light containing some red light is desirable. Some of the Al in the YAG:Ce³⁺, is often replaced with Ga³⁺ to form $Y_3(AlGa)_5O_{12}:Ce^{3+}$ due to the similarity in cation size to get the red light component in LEDs [3]. Knowing properties of this phosphor in detail could lead to the application of this phosphor in manufacturing of LEDs for home lighting. In this work the $Y_3(AlGa)_5O_{12}:Ce^{3+}$ powder phosphor is characterized with different techniques.

2. Experimental

In this study a commercial $Y_3(AlGa)_5O_{12}:Ce^{3+}$ powder phosphor was obtained from Phosphor Technology with CIE coordinates: (x= 0.306, y=0.521) [2]. By using X-ray Diffraction (XRD) the powder was characterized for its phase purity and crystallinity. A Bruker AXS D8ADVANCE X-ray diffractometer was used to carry out the XRD analysis. Scanning electron microscope (SEM) images of the powder were captured using a Shimadzu Superscan SSX-500 SEM system. Photoluminescence (PL) properties of the phosphor were recorded using the Carry eclipse spectrophotometer at room temperature with a monochromatized Xenon flash lamp as an excitation source. The UV-VUV excitation and emission spectra of the $Y_3(AlGa)_5O_{12}:Ce^{3+}$ were recorded between 100 to 330 nm and 252 nm, respectively, by using the UV-VUV synchrotron radiation facility at the SUPERLUMI beamline I of HASYLAB (Hamburger Synchrotron strahlungslabor) at DESY (Deutsches Elektronen-

¹ To whom any correspondence should be addressed.

Synchrotron, Hamburg, Germany) [6]. The spectra were recorded at room temperature. The setup consisted of a 2-m McPherson type primary (excitation) monochromator with a resolution up to 0.02 nm. The UV-VUV excitation spectra were corrected for the variation in the incident flux of the excitation beam using the excitation spectrum of sodium salicylate as a standard.

3. Results

The XRD pattern of $Y_3(AlGa)_5O_{12}:Ce^{3+}$ reveals a cubic polycrystalline phase with the main peak centered at $2\theta = 32.9^\circ$. The pattern corresponds to the cubic phase in the reference data ICSD No 029250. Using Scherrer's equation and the XRD peaks, the average crystal size of the phosphor was estimated to be around 80 nm.

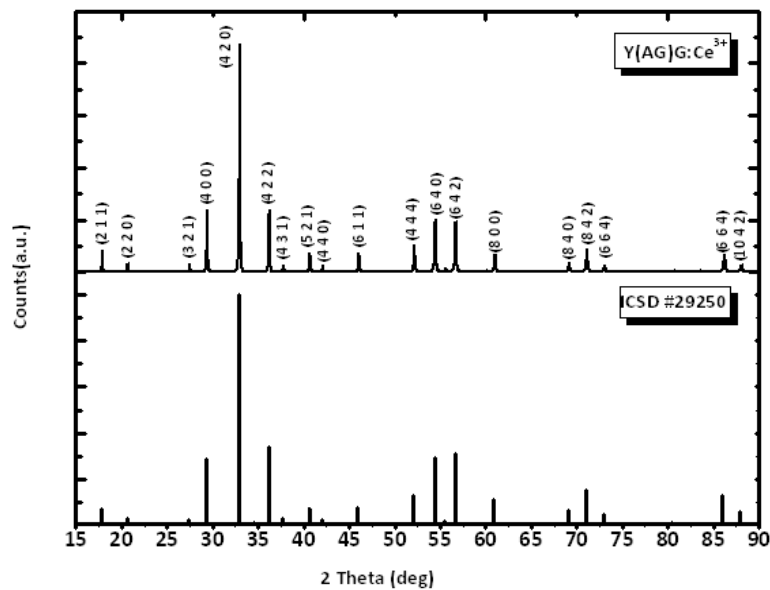


Figure 1. XRD pattern of phosphor and the ICSD reference profile.

The microstructure of $Y_3(AlGa)_5O_{12}:Ce^{3+}$ was characterized from SEM micrographs. As shown in the images, $Y_3(AlGa)_5O_{12}:Ce^{3+}$ phosphor was made up of an agglomeration of faceted spherical particles. The particle sizes were ranging from 0.5 μm to 1.4 μm .

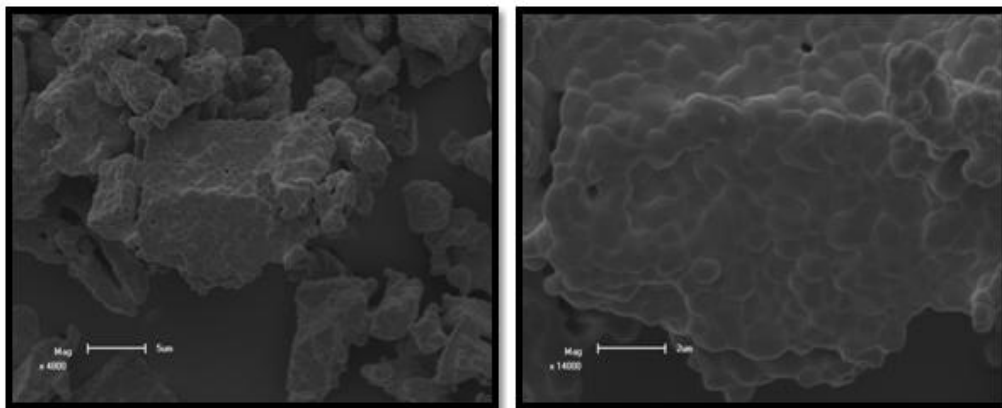


Figure 2. SEM images of the commercially obtained $Y_3(AlGa)_5O_{12}:Ce^{3+}$ phosphor.

The PL excitation and emission spectra of the $Y_3(\text{AlGa})_5\text{O}_{12}:\text{Ce}^{3+}$ phosphor are shown in figure 3. The excitation peaks are due to the 4f to 5d transitions of electrons in the Ce^{3+} ion and the emission spectra is attributed to the de-excitation of these electron from the lowest 5d level to the field split 4f levels. Shifts in the PL emission spectra are an indication of structural changes caused by the substitution of Al with Ga in the phosphor host. Table 1 shows emission data with different concentrations of Ga in the Ce^{3+} doped garnets [3]. From the table and the PL spectra in figure 3 it can be estimated that there is roughly 60% Ga and 40% Al in the $Y_3(\text{AlGa})_5\text{O}_{12}:\text{Ce}^{3+}$ crystal structure and also table 1 shows the shift in the emission and excitation wavelength as Al is substituted for Ga within the phosphor host. When Al^{3+} is substituted with Ga^{3+} , the Ga-O bonds re-adjust due to the difference in atomic radius of Ga^{3+} which is larger than Al^{3+} . The schematics of the relative arrangement of Y, O, Al and Ga were drawn using the diamond crystal software [4] and are shown in figure 4. The Y/Ce ions are surrounded by O^{2-} ions in the dodecahedral arrangement. The Al^{3+} and Ga^{3+} are surrounded by O^{2-} ions in a tetrahedral and octahedral arrangement. Ultimately, the substitution of Ga into the YAG lattice resulting in a decompression of oxygen atoms directly coordinated to the Ce^{3+} atom and the structure becomes more cubic. This change in structure directly affects the 5d orbitals of the Ce^{3+} and likewise the PL characteristics [3].

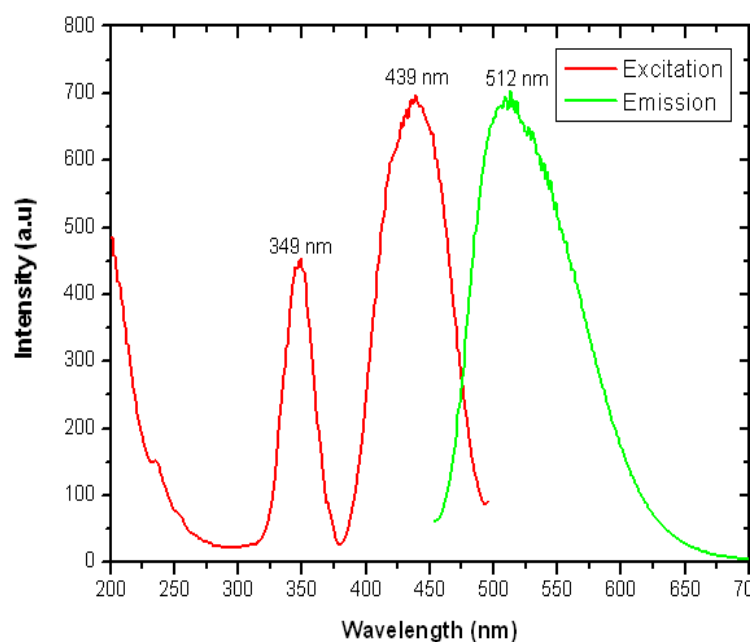


Table 1. Spectroscopic and structural properties of Ce^{3+} doped garnets [3]

| Host | $\lambda_{\text{ex}}(\text{nm})$ | $\lambda_{\text{em}}(\text{nm})$ |
|--|----------------------------------|----------------------------------|
| $Y_3\text{Al}_5\text{O}_{12}$ | 457 | 540 |
| $Y_3\text{Al}_4\text{GaO}_{12}$ | 447 | 527 |
| $Y_3\text{Al}_3\text{Ga}_2\text{O}_{12}$ | 440 | 523 |
| $Y_3\text{Al}_2\text{Ga}_3\text{O}_{12}$ | 430 | 512 |
| $Y_3\text{AlGa}_4\text{O}_{12}$ | 422 | 504 |

Figure 3. PL spectra of $Y_3(\text{Al,Ga})\text{O}_{12}:\text{Ce}^{3+}$

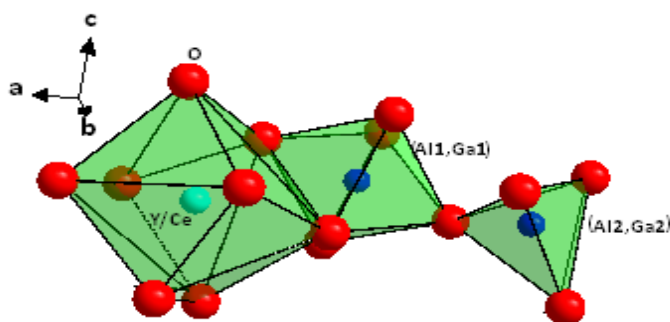


Figure 4. The relative arrangement of Y, O, Al and Ga in $Y_3(\text{AlGa})_5\text{O}_{12}:\text{Ce}^{3+}$

Figure 5 shows the relative placement of the 5d orbitals in $Y_3Al_5O_{12}:Ce^{3+}$ (YAG: Ce) and $Y_3(AlGa)_5O_{12}:Ce^{3+}$ (YAGG:Ce). Electrons are excited to the E'' state of the 5d orbital and are emitted from the E' state. The splitting of the E'' and E' states is determined by the crystal field around the Ce^{3+} atom. In unsubstituted YAG, the oxygen atoms around the Ce^{3+} atom are highly compressed and form a non cubic structure. The splitting of the E'' and E' states increases as the oxygen atoms are further distorted from the cubic structure. As Ga is substituted into YAG, oxygen atoms surrounding the Ce^{3+} atom are decompressed and form a cubic structure. As a result, the splitting between the E'' and E' states decreases with the Ga content. Consequently, the samples with Ga have noticeably shorter emission wavelengths (higher energy) [5].

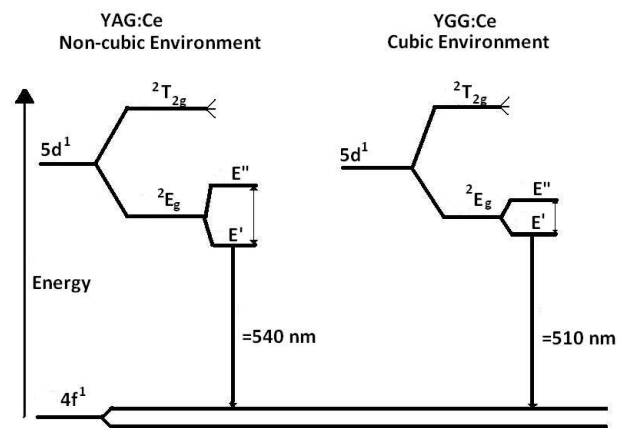


Figure 5. Energy level diagram for YAG: Ce and YAGG:Ce (not drawn to scale)[5]

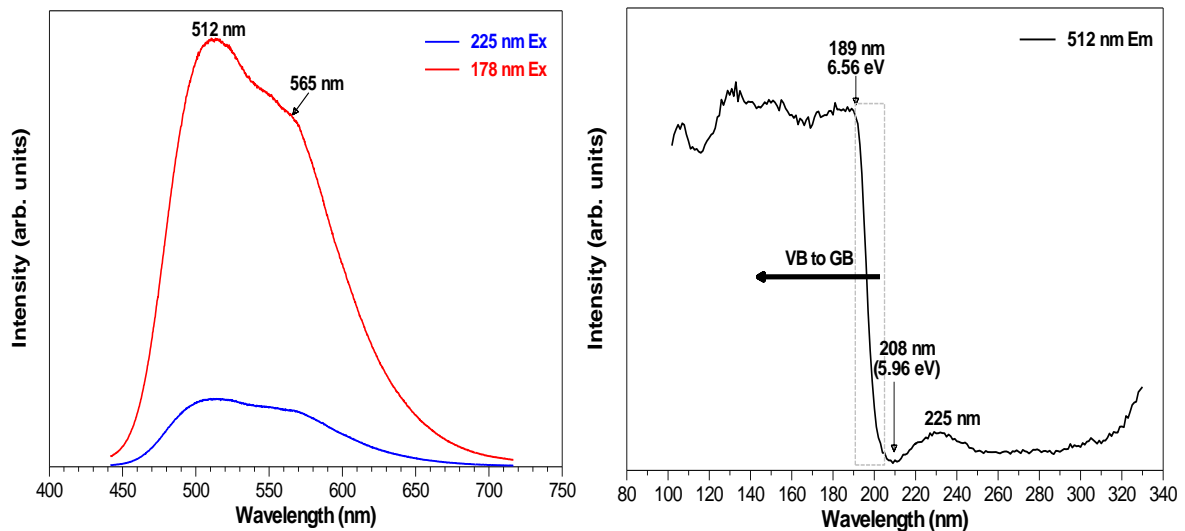


Figure 6. The emission and excitation spectra of the $Y_3(AlGa)_5O_{12}:Ce^{3+}$ phosphor measured with an excitation wavelengths of 178 and 225 nm and at an emission wavelength of 512 nm.

At room temperature, undoped YAG has a transmission window from the end of the lattice multiphonon bands at 4.2 μm to the beginning of the UV region at about 300 nm. Consequently YAG

is transparent and colorless in the visible range. YAG's optical band gap is in the order of 6.6 eV, with the valence band comprised of filled oxygen 2p orbitals, and the conduction band comprised of empty yttrium 4d orbitals. The UV absorption between 300 nm and the band edge at 190 nm varies dramatically from crystal to crystal [7]. YAG:Ce³⁺ mainly belongs to the luminescent materials with individual luminescent centers. The Ce³⁺ ion has only one electron in the 4f state. The ground state is split into a ²F_{5/2} and a ²F_{7/2} level by the spin-orbit interactions. The first excited state originates from the 5d state, which interacts strongly with the host lattice due to the large spatial extent of the 5d wave function. Thus the crystal-field interaction dominates over the spin-orbit interaction and the 4f to 5d transitions are parity and spin allowed [8]. When a Ce³⁺ ion enters exclusively one specific lattice site, its 5d state will be split into 2–5 different components depending on the site symmetry [9]. The 5d state may also split into several more components if present in more than one lattice position with different site symmetry. Coetsee et. al. [10] found that the cathodoluminescent (CL) and PL emission spectra for Y₂SiO₅:Ce³⁺ phosphor powder due to the Ce³⁺ ions were attributed to the two different sites (A1 and A2) of the Ce³⁺ ion in the host matrix and the difference in the orientation of the neighbor ions in the complex crystal structure. Each Ce³⁺ site gave rise to transitions from the 5d to the two (therefore two peaks) 4f energy levels (²F_{5/2} and ²F_{7/2} due to crystal field splitting). For the understanding of the lanthanide fd structure, knowledge about the excitation spectrum of the Ce³⁺ ion in a certain host lattice is very important. The Ce³⁺ ion has the 4f¹ configuration, and irradiation with UV radiation will excite this 4f electron into a 5d orbital, leaving the 4f shell empty. Therefore, the excitation spectrum of Ce³⁺ will give direct information on the crystal-field splitting of the 5d orbitals. A similar crystal-field splitting is expected for all rare-earth ions in the same host lattice. The crystal-field splitting of the 5d states dominates the structure in the fd excitation spectra, even in the more complex rare-earth ions with more than one 4f electron cases [11].

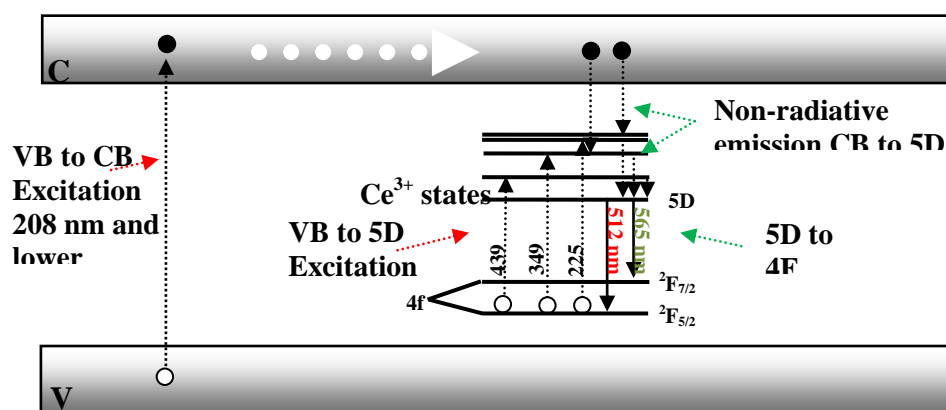


Figure 7. The energy diagram of the Y₃(AlGa)₅O₁₂:Ce³⁺ phosphor showing the excitation and emission as compiled from the emission and excitation spectra.

The emission spectra of Y₃(AlGa)₅O₁₂:Ce³⁺ were obtained under excitation of the host at 178 nm and 225 nm at room temperature (Figure. 6). Except for the intensity difference the spectra are identical with a broad peak consisting of two peaks at around 512 and 565 nm. These peaks are from the de-excitation of electrons from the lowest 5d level to the field split 4f (²F_{5/2} and a ²F_{7/2}) levels. Similar emission spectra were obtained with excitation wavelengths of 349 and 439 nm, figure. 3. The two emission peaks confirm the arrangement of the atoms in which the Ce³⁺ can only occupied one site position, as shown in figure 4. The excitation spectra shown in Figure 3 and 6 were measured from the 512 nm emission. Excitation peaks were obtained at 349, 439, 225 and 189 nm. The last peak started to increase from 209 nm up to 189 nm is assigned to the host-related absorption, since many phosphors show host-related absorptions around this spectral range [9]. In this case it is an indication of the band gap absorption of the Y₃(AlGa)₅O₁₂ between 5.96 eV (208 nm) and 6.56 eV (189 nm). The

other excitation peaks clearly indicate the excitation peaks of the 4f ($^2F_{7/2}$) to 5D levels. It is therefore clear that the Ce^{3+} is excited via the conduction band as well as in the Ce^{3+} ion itself. A summary of the energy levels of Ce^{3+} in the $Y_3(AlGa)_5O_{12}$ is given in figure 8 as obtained and compiled from the measured excitation and emission spectra. The Ce^{3+} energy values of the 5d lines obtained from this study compared very well with that obtained by Tomiki et. al. [12]. The values from Tomiki are: 460 nm (2.695 eV); 340 nm (3.643 eV); 266 nm (4.66 eV); 228 nm (5.44 eV) and 204 nm (6.07 eV).

4. Conclusions.

Ga substitution induced changes in the crystal structure of $Y_3Al_5O_{12}:Ce^{3+}$, these changes are observed in the morphological and luminescence properties. Samples with Ga have noticeably shorter emission wavelength (higher energy) and the absorption wavelengths are longer (lower energy). The excitation peaks indicated that Ce^{3+} is excited via the conduction band as well as in the Ce^{3+} ion itself. The two emission peaks confirmed the arrangement of the atom in which the Ce^{3+} can only occupy one lattice site position.

Acknowledgements.

For UV-VUV measurements, a special thanks to the synchrotron radiation facility at the SUPERLUMI beam line I of HASYLAB (Hamburger Synchrotron strahlungslabor) at DESY (Deutsches Elektronen-Synchrotron, Hamburg, Germany). The National Research Foundation and the University of the Free State for financial support.

References

- [1] Schotter P, Schmidt R and Schneider J 1997 *Appl. Phys. A* **64** 417-418
- [2] <http://www.phosphor-technology.com/products/crt.htm> [Accessed 29 May 2012].
- [3] Wu J L, Gundiah G and Cheetham A K 2007 *Structure-property correlations in Ce-doped garnet phosphors for use in solid state lighting* (Chemical Physics Letters vol 441) pp 250-254
- [4] K. Brandenburg, DIAMOND-3.0e, Visual crystal structure information System, Crystal impact distribution, Bonn, Germany, 1998
- [5] Hansel R, Allison S and Walker G 2010 *J Mater Sci* **45** 146-150
- [6] HASYLAB, Beamline I: SUPERLUMI, http://hasylab.desy.de/facilities/doris_iii/beamlines/i_superlumi (accessed on Jan. 2012)
- [7] Kuo J and Chen W 1987 *The electrical and optical properties of doped Yttrium Aluminium Garnets* (PhD thesis University of California, Berkeley) p 77
- [8] Xin F, Zhao S, Xu S, Jia G, Deng D, Wang H and Huang L 2012 30(1) 21-24.
- [9] Wang Y, Zhang J, Hou D, Liang H, Dorenbos P, Sun S and Tao Y 2012 *Optical Materials* **34** 1214–1218
- [10] Coetsee E, Terblans J J, Ntwaeaborwa O M and Swart H C 2009 *Physica B Physics of Condensed Matter* 404 (22) 4426 - 4430.
- [11] van Pieterse L, Reid M F, Wegh R T, Sovarna S and Meijerink A 2002, *Physical Review. B* **65** 045113
- [12] Tomiki T, Akamine H, Gushiken M, Kinjoh Y, Miyazato M, Miyazato T, Toyokawa N, Hiraoka M, Hirata N, Ganaha Y and Futemma T 1991 *J. Phys. Soc. Jpn.* 60(7), 2437– 2445